Electronic Supplementary Material (ESI) for New Journal of Chemistry.

Supplementary Information

Structural reorganization in a hydrogen-bonded organic framework

Javier Castells-Gil, Natalia M. Padial, and Carlos Martí-Gastaldo

Instituto de Ciencia Molecular, Universitat de València, Catedrático José Beltrán 2, 46980, Paterna (Spain).

E-mail: carlos.marti@uv.es

Table of contents:

SI1. Chemical Characterization of compound 1

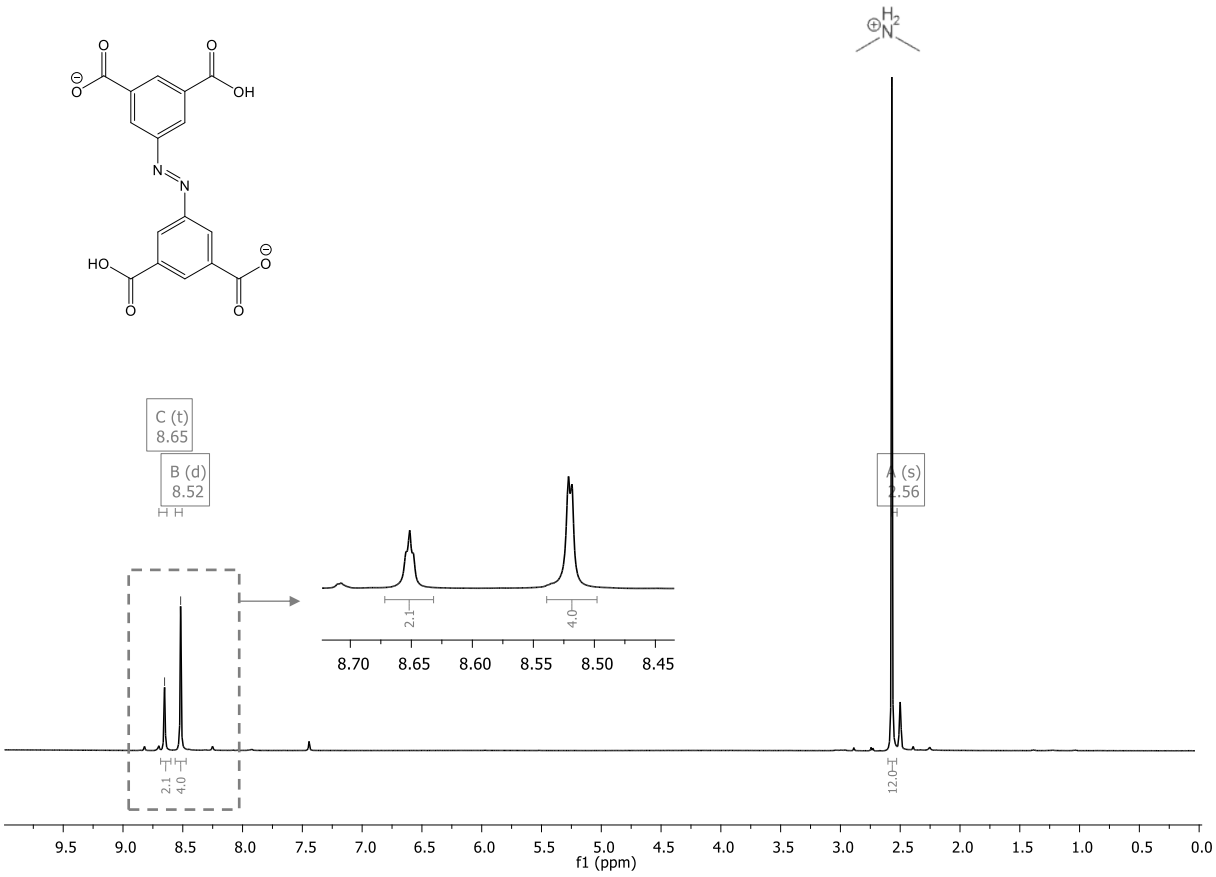

Figure SI1. ^{1}H-NMR spectrum of compound **1**, $[H_2abtc][DMA]_2$

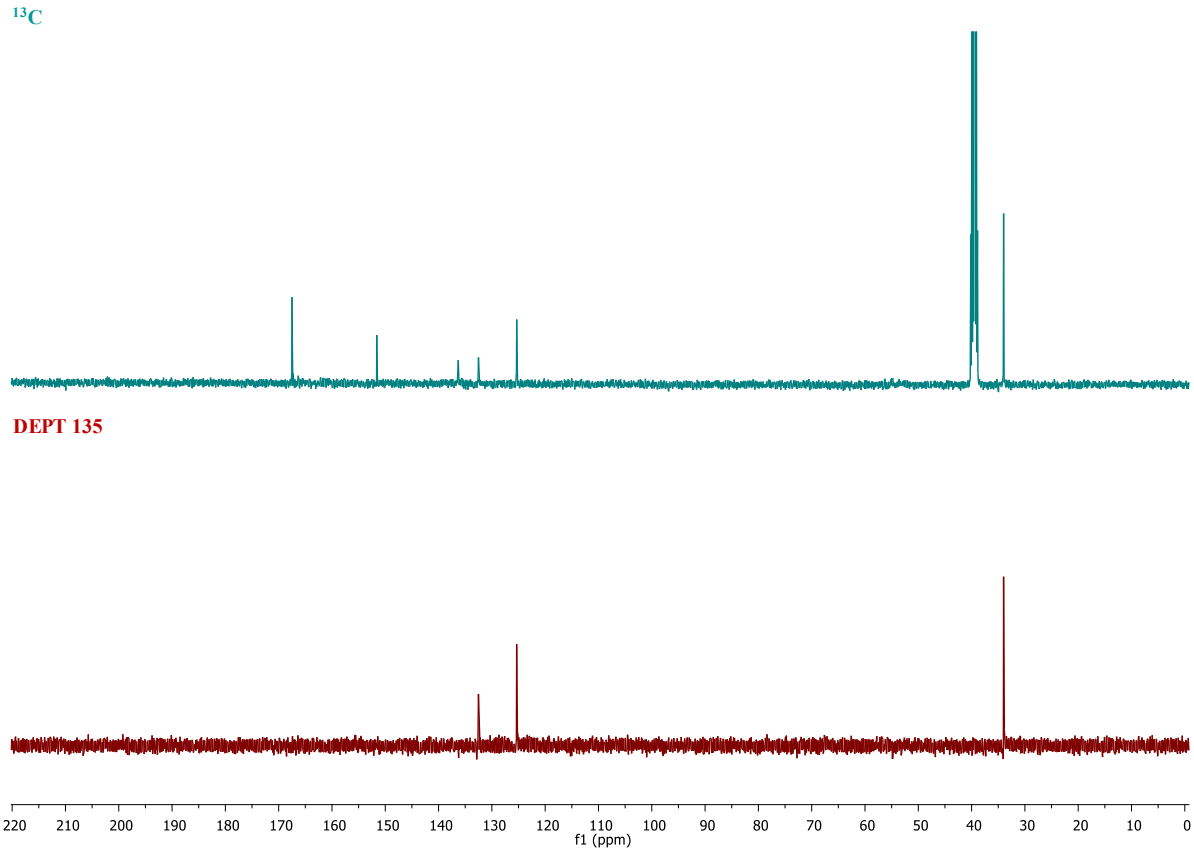

Figure SI2. ^{13}C NMR (blue) and DEPT-135 NMR (red) of **1**

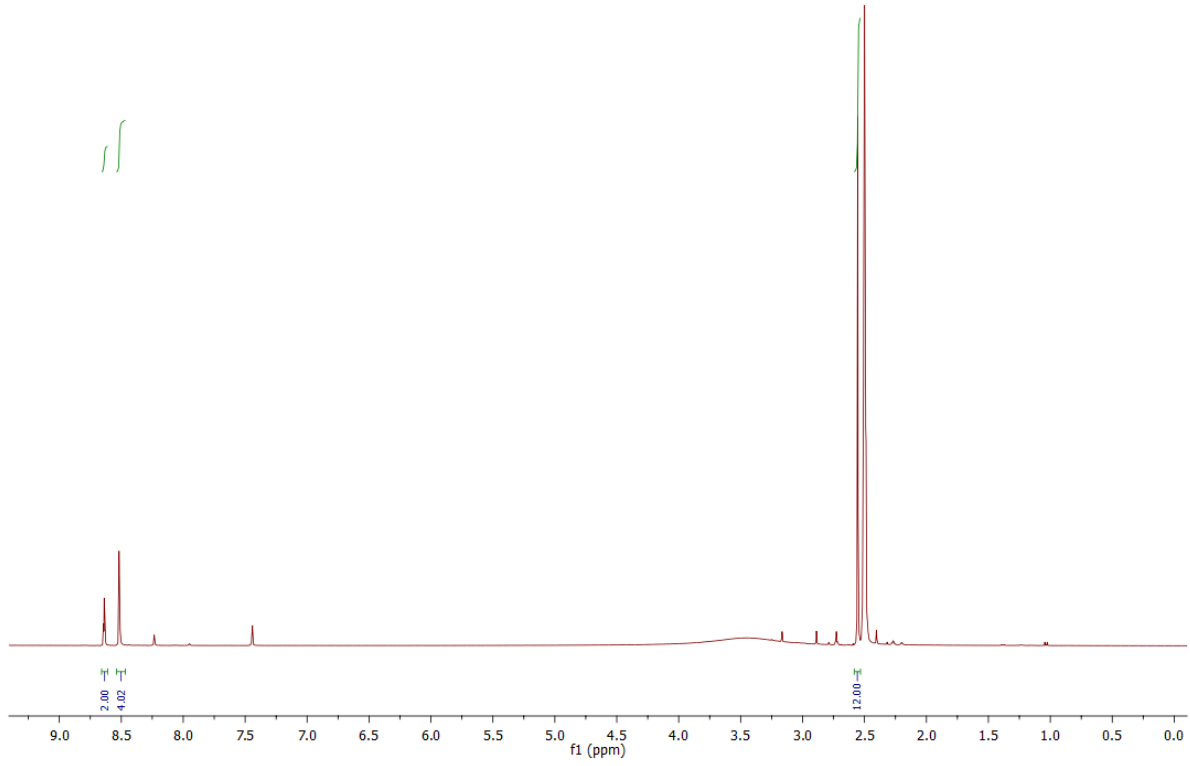

Figure SI3. ^{1}H-NMR spectrum in DMSO of compound **1** after soaking in MeOH for 1 week

SI2. NMR experiments

In a typical experiment, 10 mg of solid were dissolved in 0.6 mL of deuterated dimethylsulfoxide (DMSO-d_6). The resulting orange solutions were directly used for NMR data collection. Due to all protons of GND^+ and $AmGND^+$ are susceptible to hydrogen–deuterium exchange, the progress of the reaction was monitored by gradual decrease of DMA^+ signal in ^1H NMR (2.58 ppm). The presence of GND^+ and $AmGND^+$ was demonstrated by the signal of imine group in ^{13}C NMR (158.5 ppm for GND^+ and 159.6 ppm for $AmGND^+$).

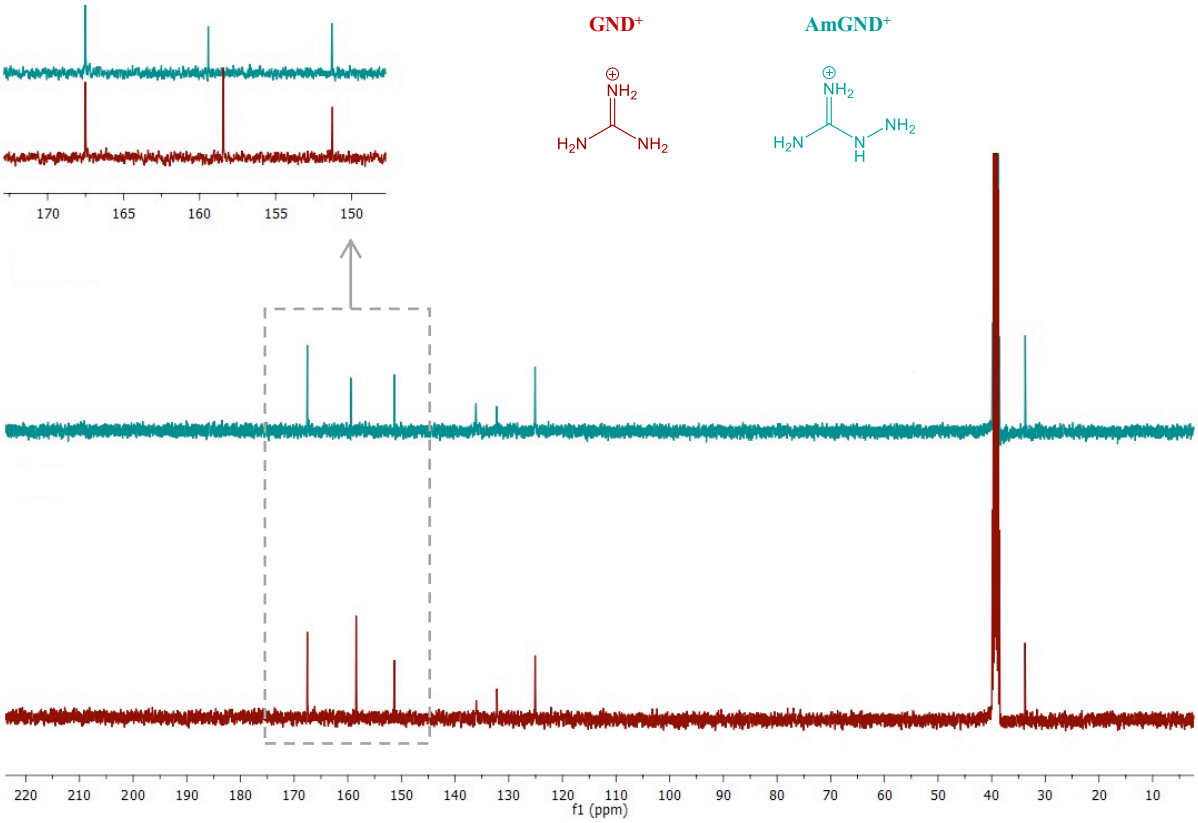

Figure SI4. Comparison of ^{13}C-NMR spectrum of **1** in GND^+ (red) and $AmGND^+$ (blue) solutions after 13 days

General procedure A for the NMR experiments of DMA^+ cation replacement

For each time, 15 mg of compound **1** was soaked in 5 mL saturated solutions of GND·HCl (0.1 mol·L^{-1}) in ethanol (96%). The solution was refreshing every day during 30 days. After that, the orange solid was washed with 5 mL of absolute ethanol for 3 times, the solvent was removed by syringe and air drying. **0.5d**: ^1H NMR (500 MHz, DMSO) δ: 8.65 (t, *J* = 1.4 Hz, 2H), 8.52 (d, *J* = 1.4 Hz, 4H), 2.58 (s, 12H). ^{13}C NMR (125 MHz, DMSO, DEPT) δ: 167.5 (C), 151.4 (C), 136.0 (C), 132.2 (CH), 125.1 (CH), 33.7 (CH_3). **1d**: ^1H NMR (500 MHz, DMSO) δ: 8.65 (t, *J* = 1.4 Hz, 2H), 8.52 (d, *J* = 1.4 Hz, 4H), 2.58 (s, 12H). ^{13}C NMR (125 MHz, DMSO, DEPT) δ: 167.5 (C), 151.4 (C), 136.0 (C), 132.2 (CH), 125.1 (CH), 33.7 (CH_3). **2d**: ^1H NMR (500 MHz, DMSO) δ: 8.65 (t, *J* = 1.4 Hz, 2H), 8.52 (d, *J* = 1.4 Hz, 4H), 2.58 (s, 12H). ^{13}C NMR (125 MHz, DMSO, DEPT) δ: 167.5 (C), 151.4 (C), 136.0 (C), 132.2 (CH), 125.1 (CH), 33.7 (CH_3). **3d**: ^1H NMR (500 MHz, DMSO) δ: 8.65 (t, *J* = 1.4 Hz, 2H), 8.52 (d, *J* = 1.4 Hz, 4H), 2.58 (s, 9.4H). ^{13}C NMR (125 MHz, DMSO, DEPT) δ: 167.7 (C), 158.5 (C), 151.4 (C), 136.0 (C), 132.2 (CH), 125.3 (CH), 33.7 (CH_3). **5d**: ^1H NMR (500 MHz, DMSO) δ: 8.65 (t, *J* = 1.4 Hz, 2H), 8.52 (d, *J* = 1.4 Hz, 4H), 2.58 (s, 5.8H). ^{13}C NMR (125 MHz, DMSO, DEPT) δ: 167.7 (C), 158.5 (C), 151.4 (C), 136.0 (C), 132.2 (CH), 125.3 (CH), 33.7 (CH_3). **7d**: ^1H NMR (500 MHz, DMSO) δ: 8.65 (t, *J* = 1.4 Hz, 2H), 8.52 (d, *J* = 1.4 Hz, 4H), 2.58 (s, 3.6H). ^{13}C NMR (125 MHz, DMSO, DEPT) δ: 167.7 (C), 158.5 (C), 151.4 (C), 136.0 (C), 132.2 (CH), 125.3 (CH), 33.7 (CH_3). **9d**: ^1H NMR (500 MHz, DMSO) δ: 8.65 (t, *J* = 1.4 Hz, 2H), 8.52 (d, *J* = 1.4 Hz, 4H), 2.58 (s, 2.4H). ^{13}C NMR (125 MHz, DMSO, DEPT) δ: 167.7 (C), 158.5 (C), 151.4 (C), 136.0 (C), 132.2 (CH), 125.3 (CH), 33.7 (CH_3). **13d**: ^1H NMR (500 MHz, DMSO) δ: 8.65 (t, *J* = 1.4 Hz, 2H), 8.52 (d, *J* = 1.4 Hz, 4H), 2.58 (s, 2.0H). ^{13}C NMR (125 MHz, DMSO, DEPT) δ: 167.7 (C), 158.5 (C), 151.4 (C), 136.0 (C), 132.2 (CH), 125.3 (CH), 33.7 (CH_3). **30d**: ^1H NMR (500 MHz, DMSO) δ: 8.65 (t, *J* = 1.4 Hz, 2H), 8.52 (d, *J* = 1.4 Hz, 4H), 2.58 (s, 2.0H). ^{13}C NMR (125 MHz, DMSO, DEPT) δ: 167.7 (C), 158.5 (C), 151.4 (C), 136.0 (C), 132.2 (CH), 125.3 (CH), 33.7 (CH_3).

Table SI1. Replacement percentage of **1** with GND^+ in ethanol

SAMPLE	Linker (8.52 ppm signal, 4H)	DMA (2.58 ppm signal, 12H)	Ratio (L:DMA)	% replacement
0.5d	4.0	12.0	1:2	0
1d	4.0	12.0	1:2	0
2d	4.0	12.0	1:2	0
3d	4.0	9.4	1:1.57	22
5d	4.0	5.8	1: 0.97	52
7d	4.0	3.6	1: 0.60	70
9d	4.0	2.4	1: 0.40	80
13d	4.0	2.0	1: 0.33	84
30d	4.0	2.0	1: 0.33	84

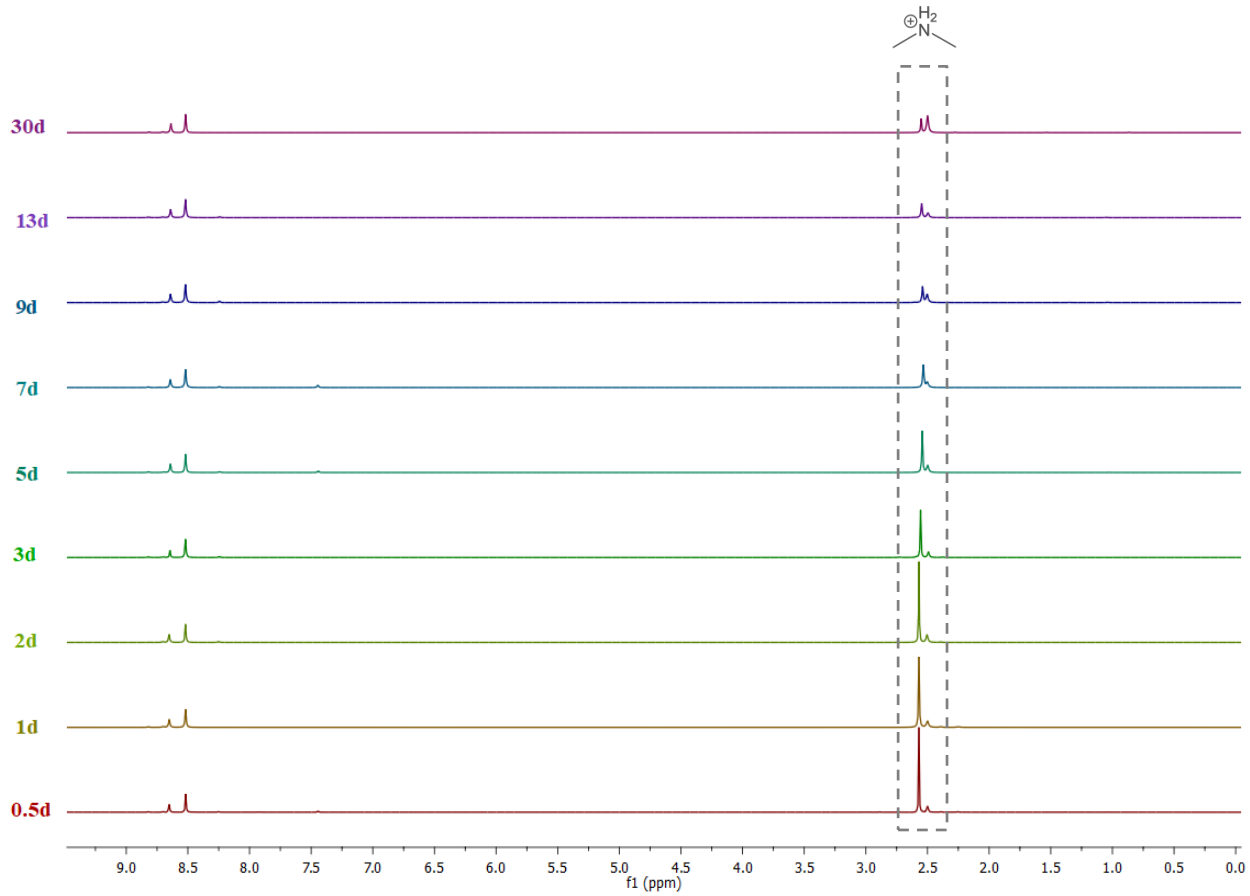

Figure SI5. ^1H NMR spectrum of DMA^+ replacement by GND^+ at different times

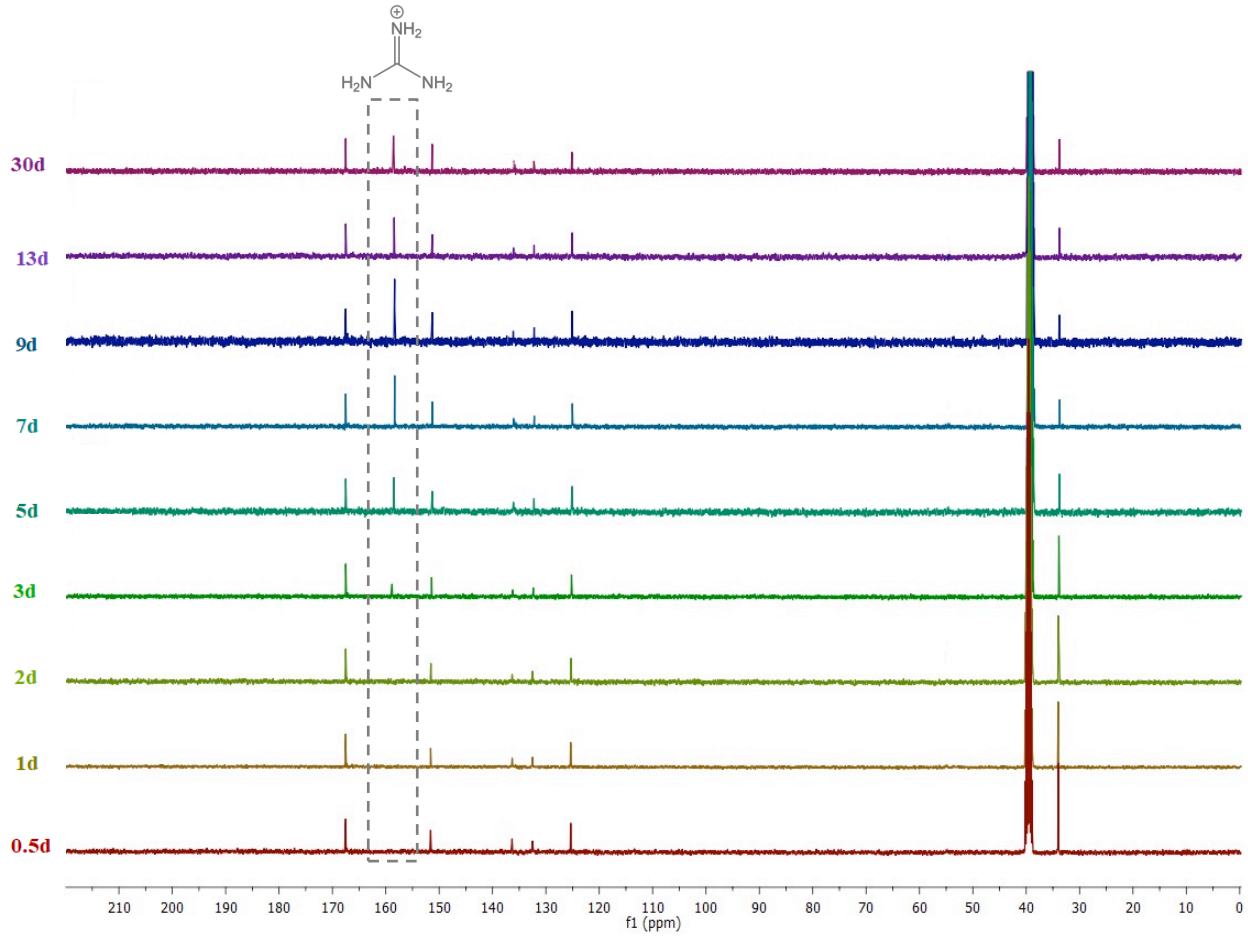

Figure SI6. ^{13}C NMR spectrum of DMA^+ replacement by GND^+ at different times

General procedure B for the DMA^+ cation replacement

For each time, 15 mg of compound **1** was soaked in 5 mL equimolar solutions of GND·HCl and AmGND·HCl (0.05 mol·L^{-1}, respectively) in ethanol (96%). The solution was refreshing every day during 60 days. After that, the orange solid was washed with 5 mL of absolute ethanol for 3 times, the solvent was removed by syringe and air drying. **1d**: ^1H NMR (500 MHz, DMSO) δ: 8.65 (t, *J* = 1.4 Hz, 2H), 8.52 (d, *J* = 1.4 Hz, 4H), 2.58 (s, 12H). ^{13}C NMR (125 MHz, DMSO, DEPT) δ: 167.5 (C), 151.5 (C), 136.1 (C), 132.2 (CH), 125.1 (CH), 33.8 (CH_3). **3d**: ^1H NMR (500 MHz, DMSO) δ: 8.65 (t, *J* = 1.4 Hz, 2H), 8.52 (d, *J* = 1.4 Hz, 4H), 2.58 (s, 10H). ^{13}C NMR (125 MHz, DMSO, DEPT) δ: 167.7 (C), 159.6 (C), 151.4 (C), 136.0 (C), 132.2 (CH), 125.3 (CH), 33.7 (CH_3). **7d**: ^1H NMR (500 MHz, DMSO) δ: 8.65 (t, *J* = 1.4 Hz, 2H), 8.52 (d, *J* = 1.4 Hz, 4H), 2.58 (s, 7.2H). ^{13}C NMR (125 MHz, DMSO, DEPT) δ: 167.7 (C), 159.6 (C), 151.4 (C), 136.0 (C), 132.2 (CH), 125.3 (CH), 33.7 (CH_3). **13d**: ^1H NMR (500 MHz, DMSO) δ: 8.65 (t, *J* = 1.4 Hz, 2H), 8.52 (d, *J* = 1.4 Hz, 4H), 2.58 (s, 5.8H).^{13}C NMR (125 MHz, DMSO, DEPT) δ: 167.7 (C), 159.6 (C), 151.4 (C), 136.0 (C), 132.2 (CH), 125.3 (CH), 33.7 (CH_3). **21d**: ^1H NMR (500 MHz, DMSO) δ: 8.65 (t, *J* = 1.4 Hz, 2H), 8.52 (d, *J* = 1.4 Hz, 4H), 2.58 (s, 5.0H). ^{13}C NMR (125 MHz, DMSO, DEPT) δ: 167.7 (C), 159.6 (C), 151.4 (C), 136.0 (C), 132.2 (CH), 125.3 (CH), 33.7 (CH_3). **30d**: ^1H NMR (500 MHz, DMSO) δ: 8.65 (t, *J* = 1.4 Hz, 2H), 8.52 (d, *J* = 1.4 Hz, 4H), 2.58 (s, 4.7H). ^{13}C NMR (125 MHz, DMSO, DEPT) δ: 167.7 (C), 159.6 (C), 151.4 (C), 136.0 (C), 132.2 (CH), 125.3 (CH), 33.7 (CH_3). **60d**: ^1H NMR (500 MHz, DMSO) δ: 8.65 (t, *J* = 1.4 Hz, 2H), 8.52 (d, *J* = 1.4 Hz, 4H), 2.58 (s, 4.2H). ^{13}C NMR (125 MHz, DMSO, DEPT) δ: 167.7 (C), 159.6 (C), 151.4 (C), 136.0 (C), 132.2 (CH), 125.3 (CH), 33.7 (CH_3).

Table SI2. Replacement percentage of DMA^+ in **1** in an equimolar mixture of $AmGND^+$ and GND^+ in ethanol

SAMPLE	Linker (8.52 ppm signal, 4H)	DMA (2.58 ppm signal, 12H)	Ratio (L:DMA)	% replacement
1	4.0	12.0	1:2	0
3	4.0	10.0	1: 1.7	15
7	4.0	7.2	1: 1.2	40
13	4.0	5.8	1: 0.97	52
21	4.0	5.0	1: 0.83	59
30	4.0	4.7	1: 0.78	61
60	4.0	4.2	1: 0.70	65

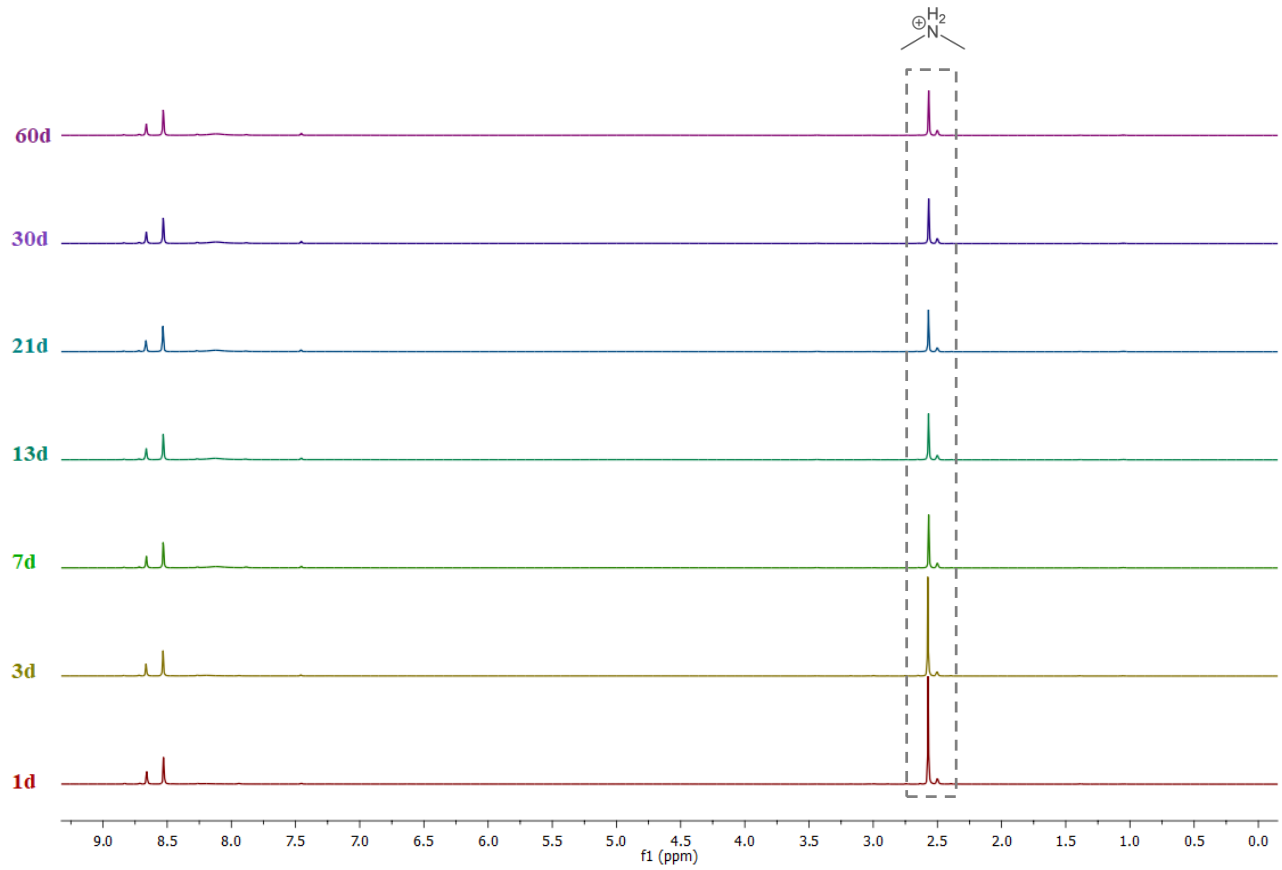

Figure SI7. ^1H NMR spectrum of DMA^+ replacement reactions of 1 with GND^+ and $AmGND^+$ cations mixtures

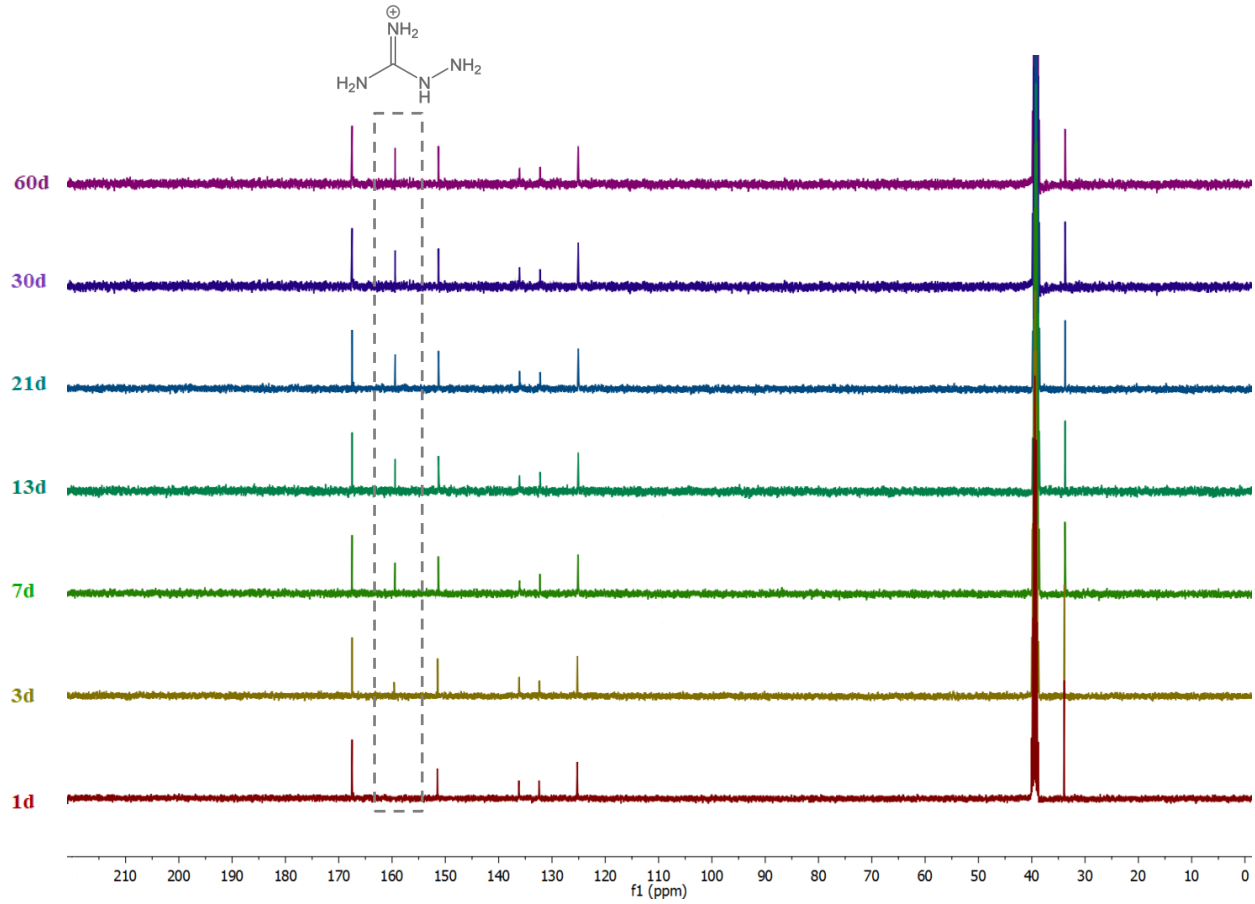

Figure SI8. ^{13}C NMR spectrum of DMA^+ replacement reactions of 1 withGND^+ and $AmGND^+$ cations mixtures

SI3. Physical characterization of compound 1

Optical microscope

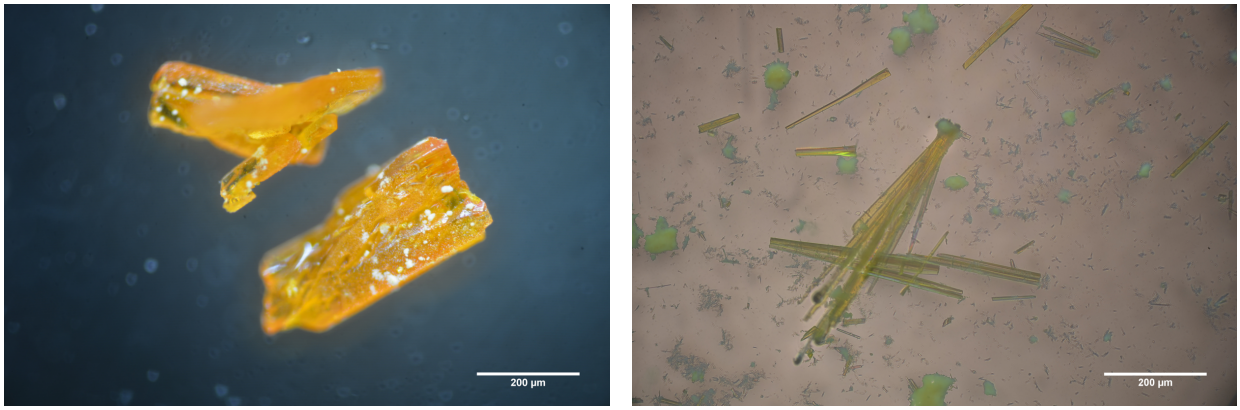

Figure SI9. Optical microscope of as-made crystals of **1** (left) and the compound **2** (right) after 10 days

Infrared spectra

FT-IR spectra of 1 in a pellet diluted with KBr measured in a FT-IR Nicolet 5700 spectrometer in the 4000–400 cm^{-1} range. (KBr, [cm^{-1}]): 1350 (m), 1430 (m), 1700 (s), 2400 (w), 2900 (w, br), 3080 (sr, br), 3440 (m, br).

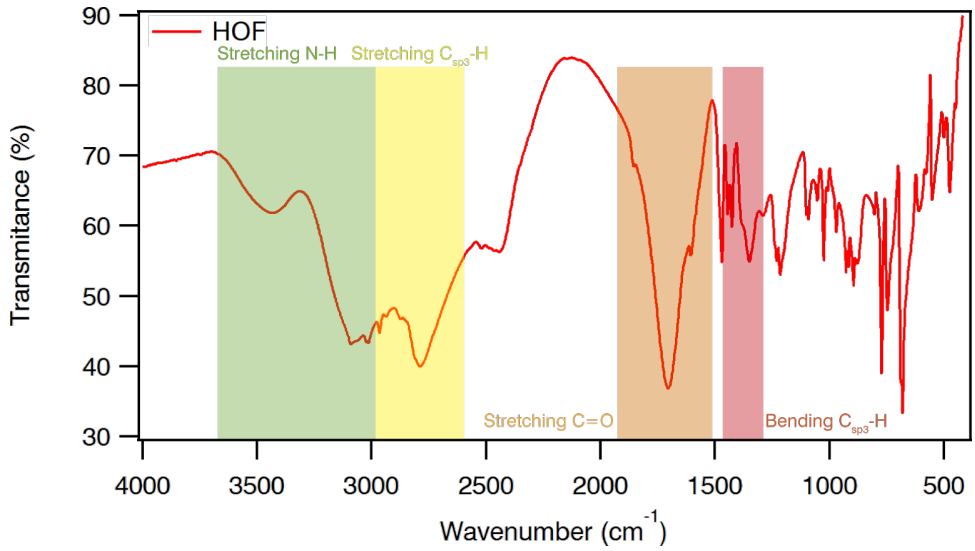

Figure SI10. FT-IR spectra of **1**

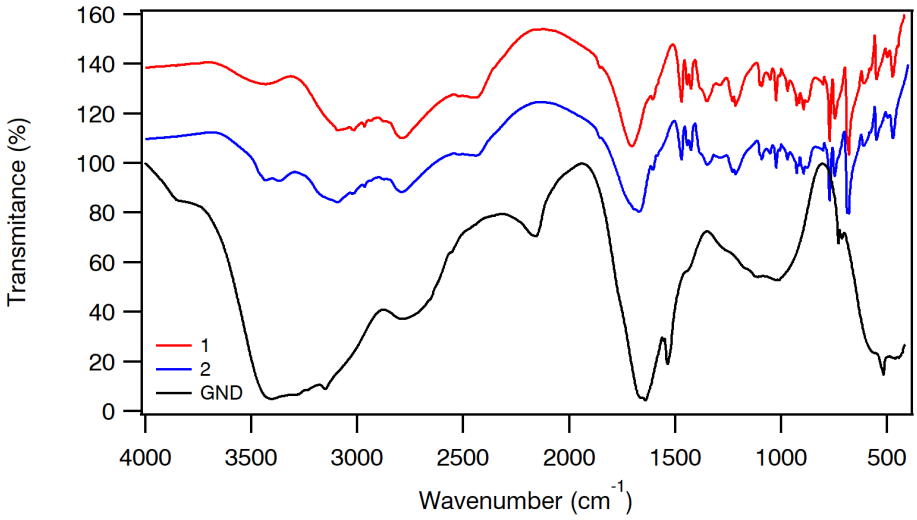

Figure SI11. FT-IR spectra of **1**, **2** and GND. The presence of N-H stretching bands around 3400cm^{-1}, not present in **1**, are indicative of the incorporation of GND to the framework in **2**.

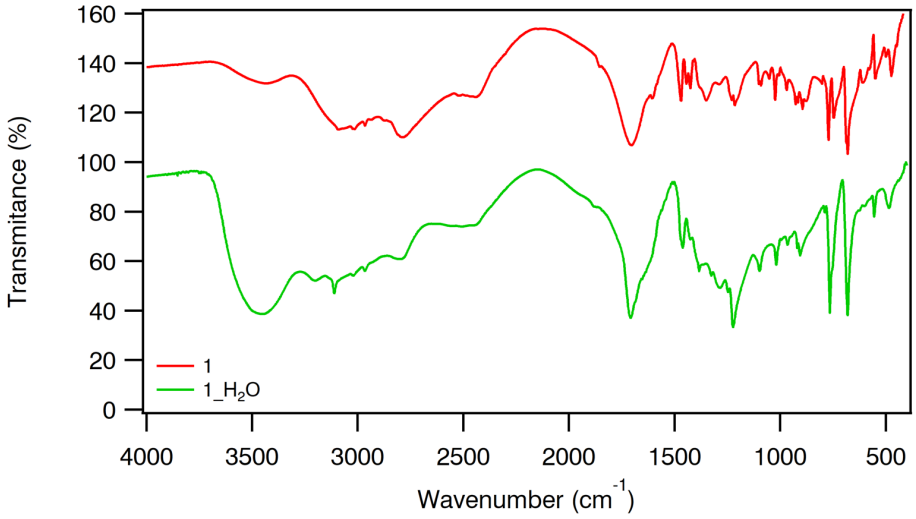

Figure SI12. FT-IR spectra of **1** and **1 in water**. The data of **1** and **1_H_2O** have been offsetted for clarity

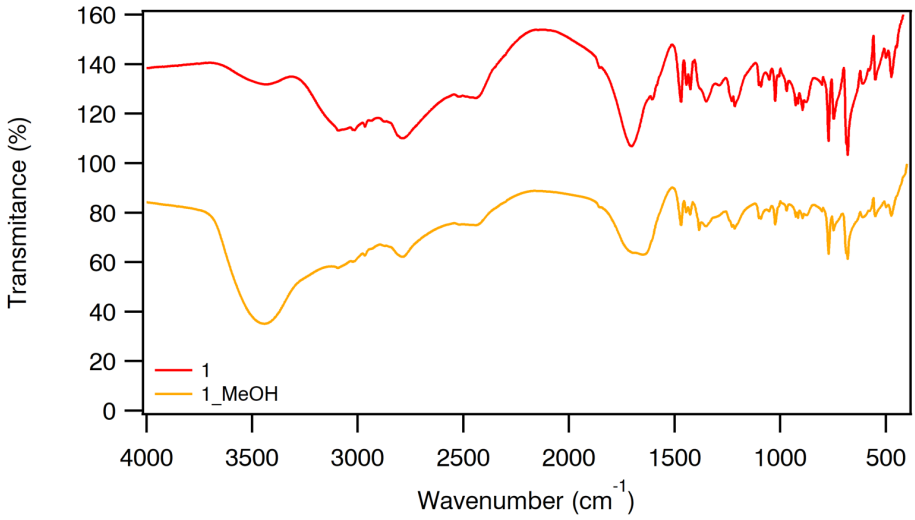

Figure SI13. FT-IR spectra of **1** and **1 in MeOH**. The data of **1** and **1_MeOH** have been offsetted for clarity

Powder X-Ray diffraction

Experimental (red dots), calculated (blue line), difference plot [(*I*obs−*I*calcd)] (black line, bottom panel) and Bragg positions (green ticks, bottom panel) for the unit cell refinement of experimental powder diffraction data of **1** collected at room temperature by using experimental single-crystal data as starting parameters. Triclinic, P-1; a = 6.0(4), b = 8.2(6), c = 10.8(8) Å; α = 74.64(4), β = 88.54(6), γ = 88.08(5)°; V = 510.78Å^3. X^2 = 1.89E-05. Snyder's FOM = 5.04. 2Theta zero shift = -0.2(2)°.

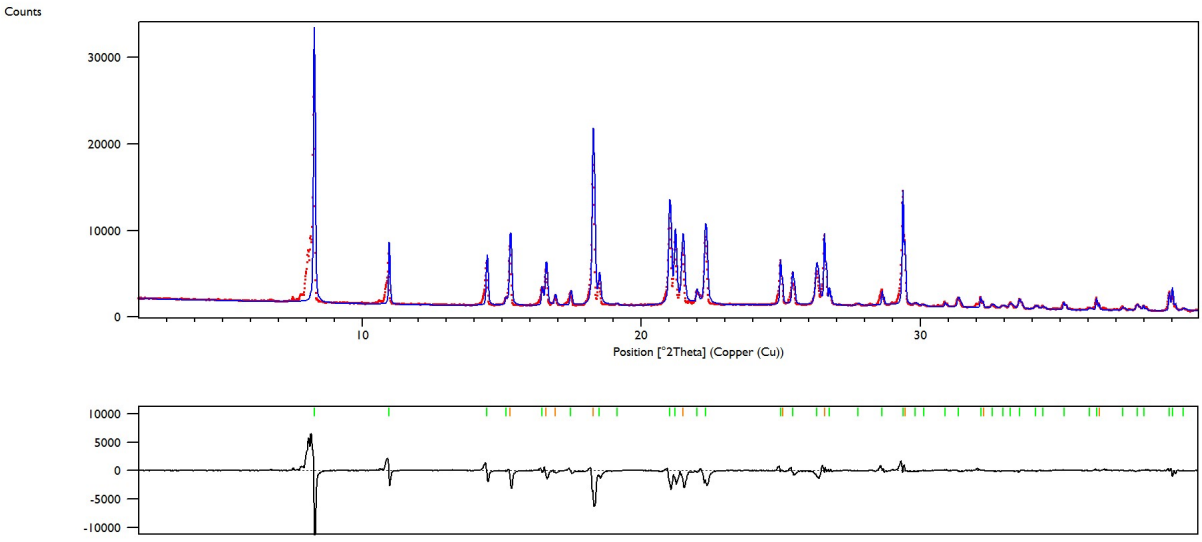

Figure SI14. PXRD of **1** and refined cell parameters calculated with X'Pert HighScore Plus

Thermogravimetric analysis

Compound **1** is thermally stable up to 200 °C where it shows a first weight loss of 20.4% close to 240 °C, that agrees well with the loss of the two molecules of dimethyl amine molecules (Calc: 20.1%). This is followed by the gradual decomposition of the framework that extends from 300 until ca. 600 °C. Thermal stability is similar to previously reported charge-assisted cation/anion hydrogen-bonded frameworks (decomposition between 240 and 300 °C).[2] In contrast, the compound **1** after being replaced with GND^+ or $AmGND^+$ shows two distinctive weight losses before decomposition at 400 °C that are ascribed to the departure of DMA and GND or AmGND molecules, respectively.

TG analysis of **1** after exposure to water shows a first weight loss of about 23% that corresponds to the loss of 12 molecules of water.

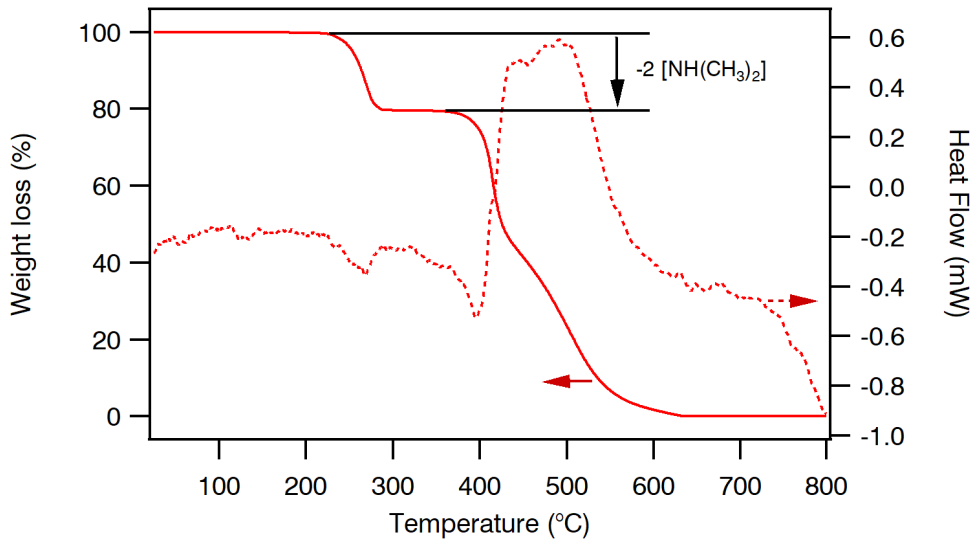

Figure SI15. TGA of **1** between 25 and 800 °C

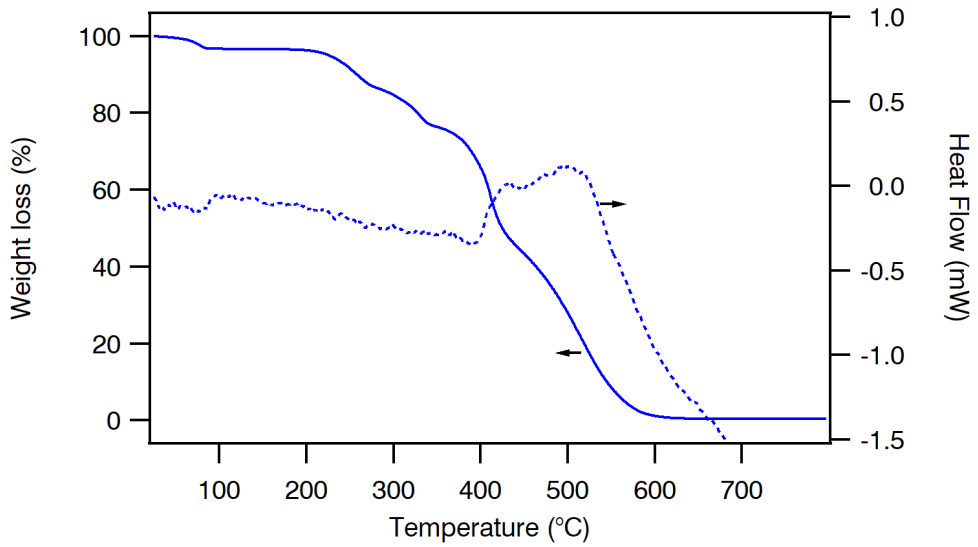

Figure SI16. TGA of **2** between 25 and 800 °C

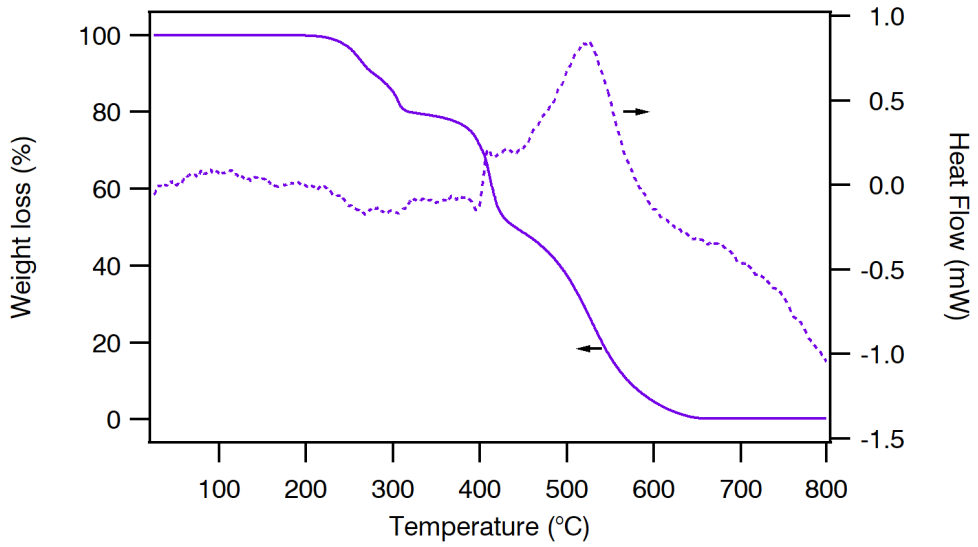

Figure SI17. TGA between 25 and 800 °C of **1** after being immersed in a $AmGND^+$ solution for 60 days.

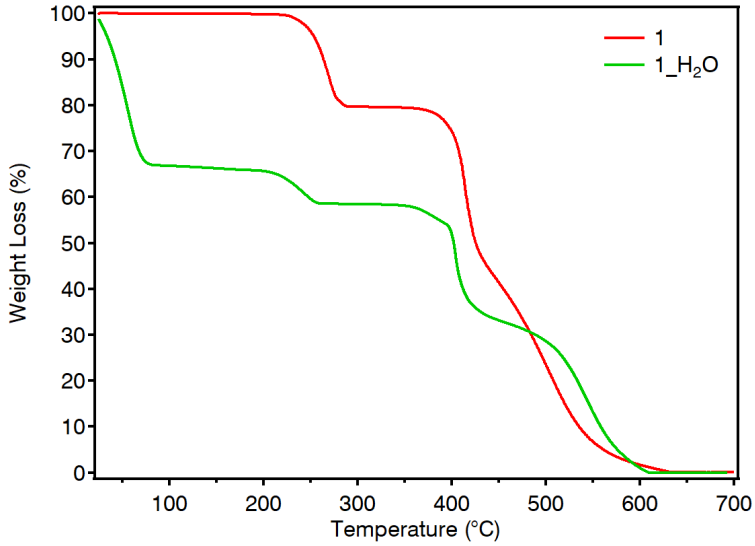

Figure SI18. TGA between 25 and 700 °C of **1** before and after being exposed to an atmosphere rich in water for several hours

Single-Crystal X-Ray diffraction

Table SI3. Crystal data and structure refinement for **1**

	1
Identification code	CCDC1576296
Empirical formula	$C_{10}H_{12}N_2O_4$
Formula weight	224.22
Temperature/K	120.00(10)
Crystal system	triclinic
Space group	P-1
a/Å	6.1091(3)
b/Å	8.2810(6)
c/Å	11.0256(7)
α/°	74.836(6)
β/°	87.904(5)
γ/°	88.263(5)
Volume/Å^3	537.87(6)
Z	2
ρ_{calc}g/cm^3	1.384
μ/mm^{-1}	0.108
F(000)	236.0
Crystal size/mm^3	0.1 × 0.1 × 0.05
Radiation	MoKα (λ = 0.71073)
2Θ range for data collection/°	6.676 to 54.836
Index ranges	-7 ≤ h ≤ 7, -10 ≤ k ≤ 10, -13 ≤ l ≤ 13
Reflections collected	5970
Independent reflections	2163 [R_{int} = 0.0350, R_{sigma} = 0.0414]
Data/restraints/parameters	2163/0/192
Goodness-of-fit on F^2	1.025
Final R indexes [I>=2σ (I)]	R_1 = 0.0424, wR_2 = 0.1022
Final R indexes [all data]	R_1 = 0.0556, wR_2 = 0.1117
Largest diff. peak/hole / e Å^{-3}	0.27/-0.24

Refinement model description: number of restraints – 0; number of constraints – 0.

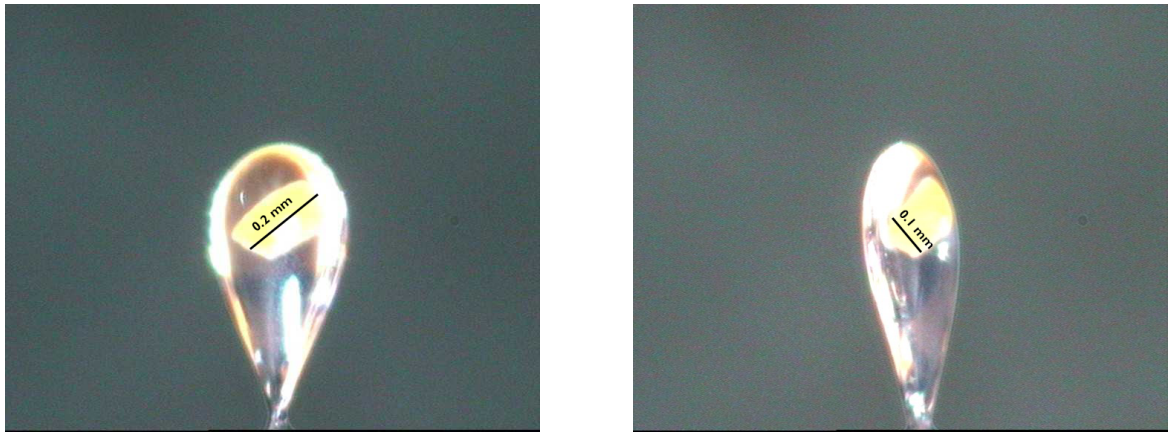

Figure SI19. Pictures for crystals of **1**

Hydrogen bonds

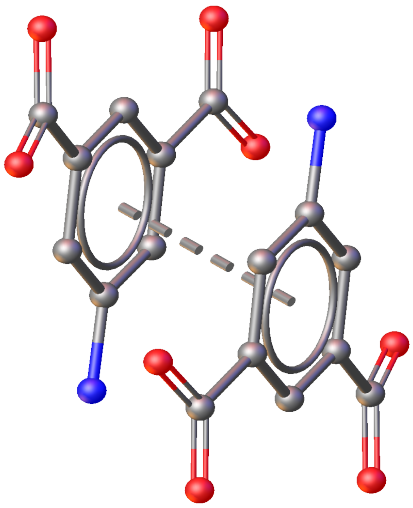

Figure SI20. Layer packing is controlled by π-π interactions between neighbouring aromatic rings that adopt a parallel arrangement with an offset of 1.3 Å and inter-centroid distance of 3.5 Å

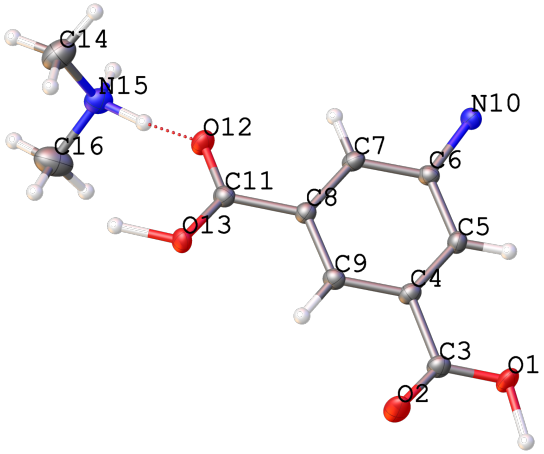

Figure SI21. Ortep representation (50% probability) of the asymmetric unit of **1**

Table SI4. Hydrogen bonds for **1**

D	H	A	d(D-H)/Å	d(H-A)/Å	d(D-A)/Å	D-H-A/°
O13	H13	O13[1]	1.24	1.24	2.476(2)	180
O1	H1	O1[2]	1.23	1.23	2.465(2)	180
N15	H15A	O12	1.01(2)	1.74(2)	2.693(2)	156(2)
N15	H15B	O2[3]	0.96(2)	1.87(2)	2.744(2)	149(2)

[1]2-X,2-Y,1-Z; [2]1-X,1-Y,-Z; [3]+X,+Y,1+Z

Unit cell refinement

Experimental (red dots), calculated (blue line), difference plot [(*I*obs−*I*calcd)] (red line, bottom panel) and Bragg positions (green ticks, bottom panel) for the unit cell refinement of experimental diffraction data of **1** collected at variable temperature (30-200 °C) by using single-crystal data available as starting parameters. PXRD patterns were collected in a PANalytical X'Pert PRO diffractometer using copper radiation (Cu Kα1 = 1.5406 Å) with an X'Celerator detector, operating at 40 mA and 45 kV. Profiles were collected in the 2° < 2θ < 60° range with a step size of 0.017°.

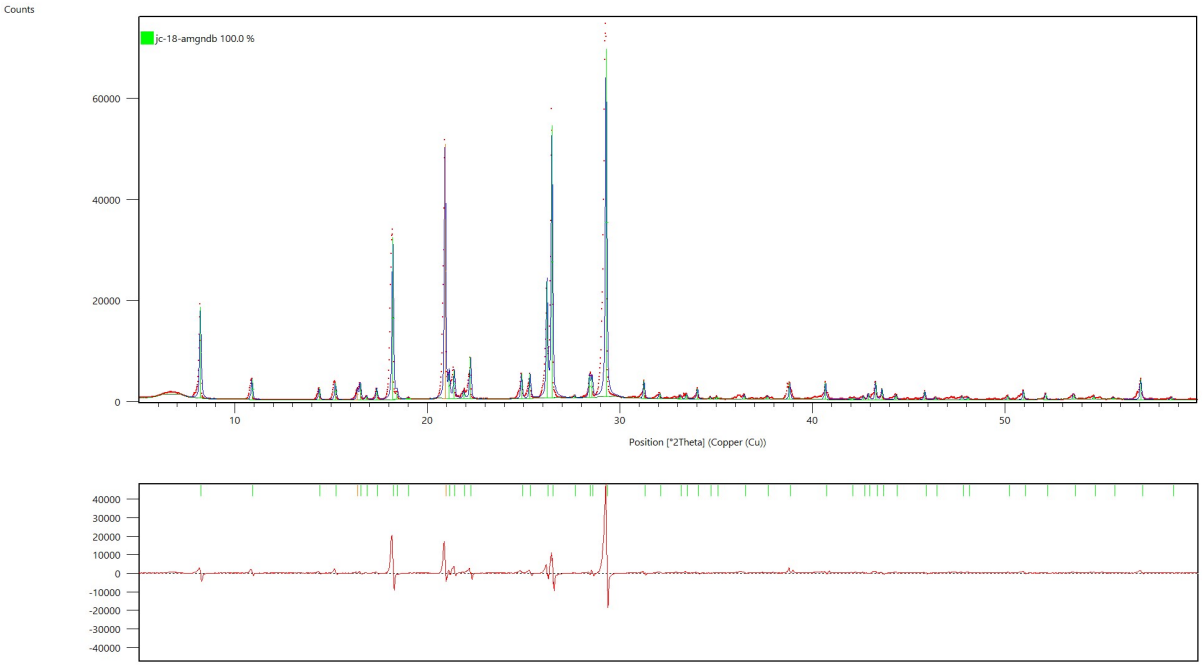

Triclinic, P-1; a = 6.1(2), b = 8.3(2), c = 11.0(3) Å; α = 74.77(2), β = 87.72(2), γ = 88.35(2) °; V = 537.55 Å^3. X^2 = 1.86E-05. Snyder's FOM = 2.4. Zero shift = -0.0(1).

Figure SI22a. Unit cell refinement of experimental diffraction data of **1** at 30 °C

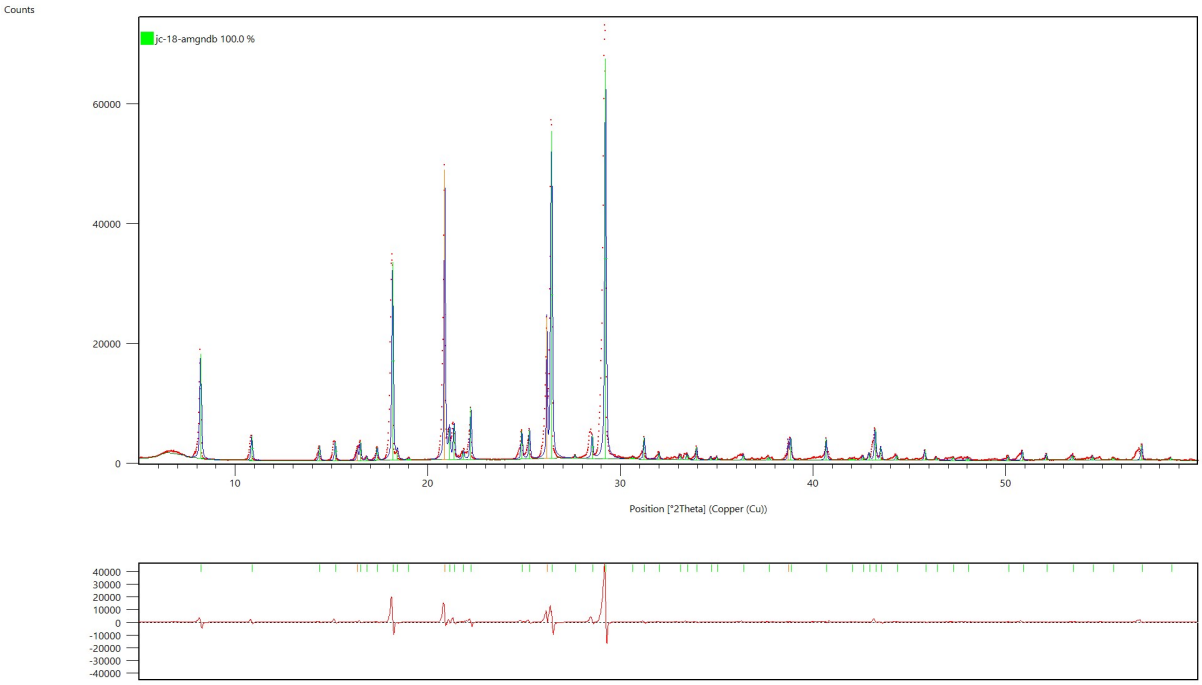

Triclinic, P-1; a = 6.1(2), b = 8.2(2), c = 10.9(4) Å; α = 74.78(2), β = 87.60(3), γ = 87.68(3) °; V = 520.55 Å^3. X^2 = 2.56E-05. Snyder's FOM = 2.0. Zero shift = -0.0(1).

Figure SI22b. Unit cell refinement of experimental diffraction data of **1** at 50 °C

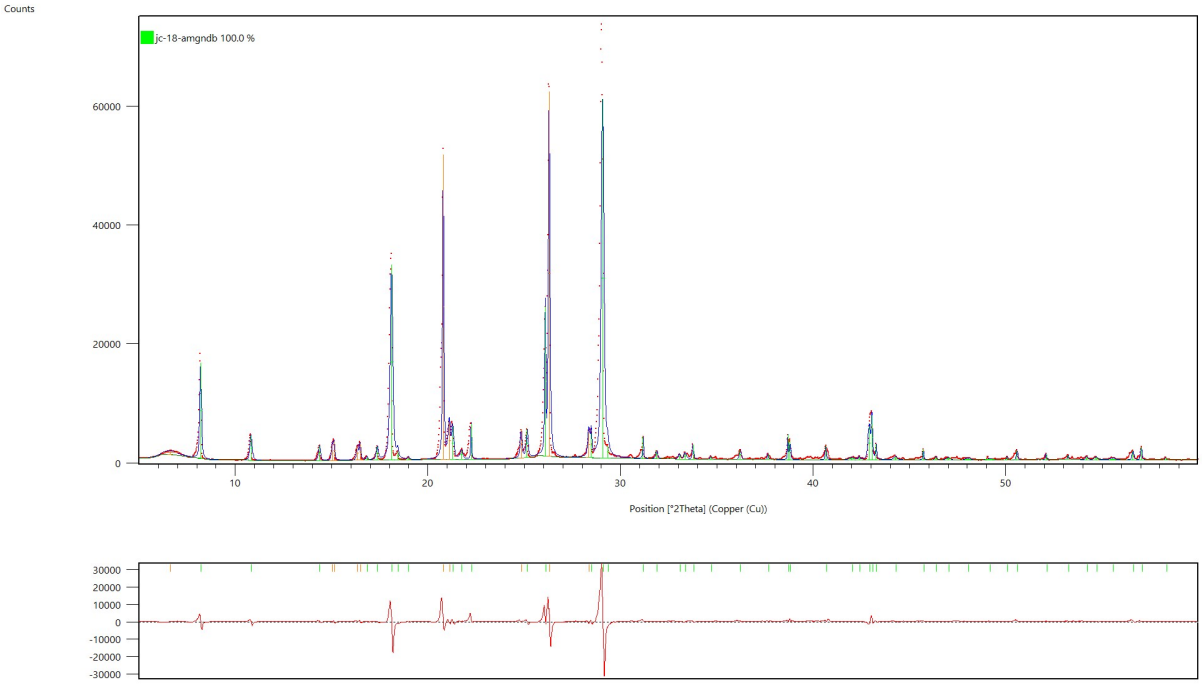

Triclinic, P-1; a = 6.0(2), b = 8.1(2), c = 10.8(3) Å; α = 74.76(2), β = 87.67(2), γ = 87.24(2) °; V = 512.38 Å^3. X^2 = 1.86E-05. Snyder's FOM = 2.3. Zero shift = -0.1(1).

Figure SI22c. Unit cell refinement of experimental diffraction data of **1** at 100 °C

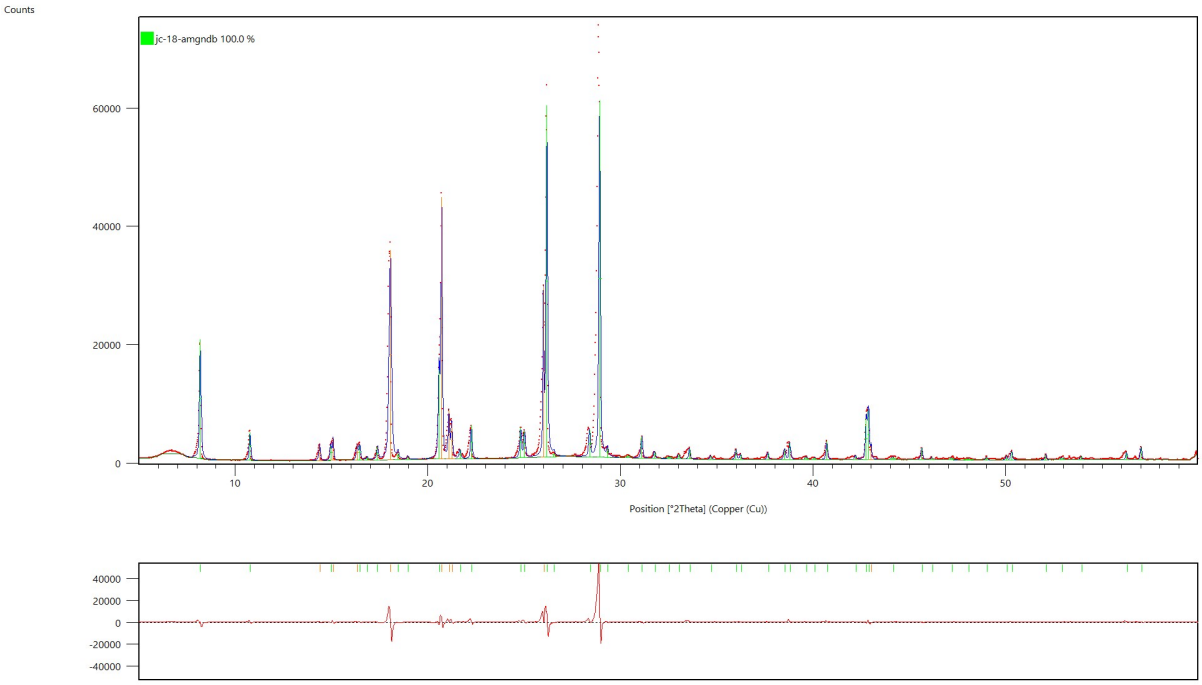

Triclinic, P-1; a = 6.0(2), b = 8.0(3), c = 10.9(5) Å; α = 75.16(2), β = 87.11(4), γ = 86.93(3) °; V = 508.01 Å^3. X^2 = 3.42E-05. Snyder's FOM = 2.2. Zero shift = 0.0(2).

Figure SI22d. Unit cell refinement of experimental diffraction data of **1** at 150 °C

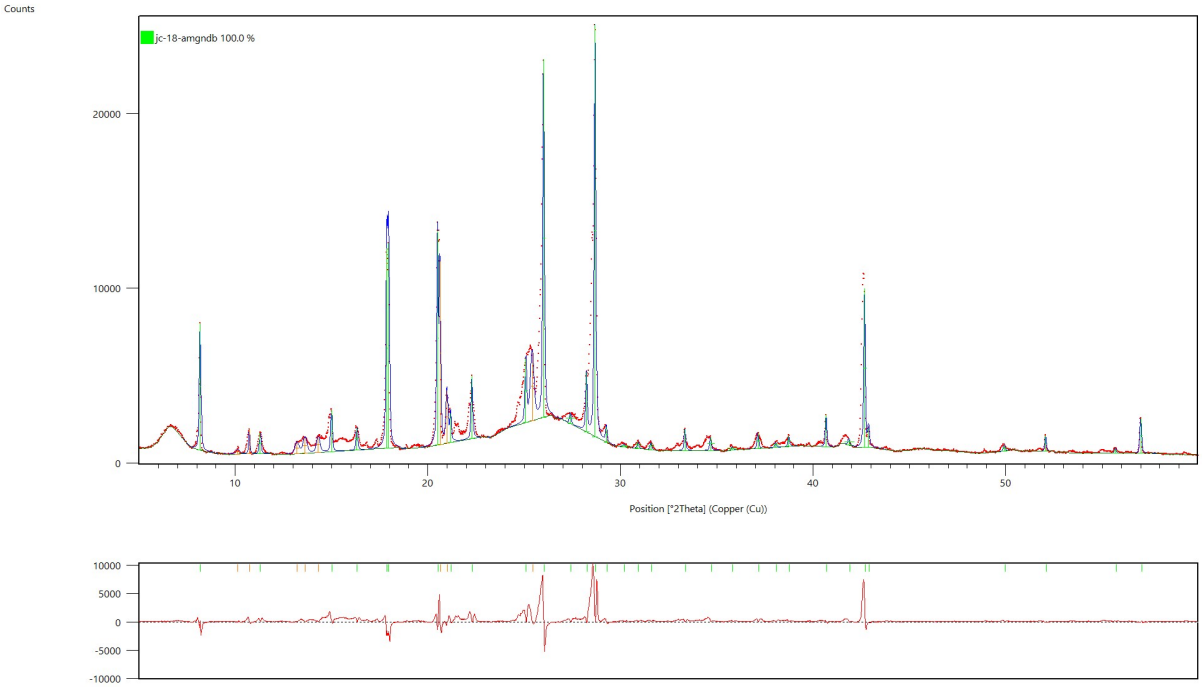

Triclinic, P-1; a = 6.0(3), b = 8.0(4), c = 11.0(6) Å; α = 74.94(3), β = 87.43(4), γ = 85.86(6) °; V = 510.69 Å^3. X^2 = 1.87E-05. Snyder's FOM = 1.4. Zero shift = 0.0(2).

Figure SI22e. Unit cell refinement of experimental diffraction data of **1** at 200 °C

Stability

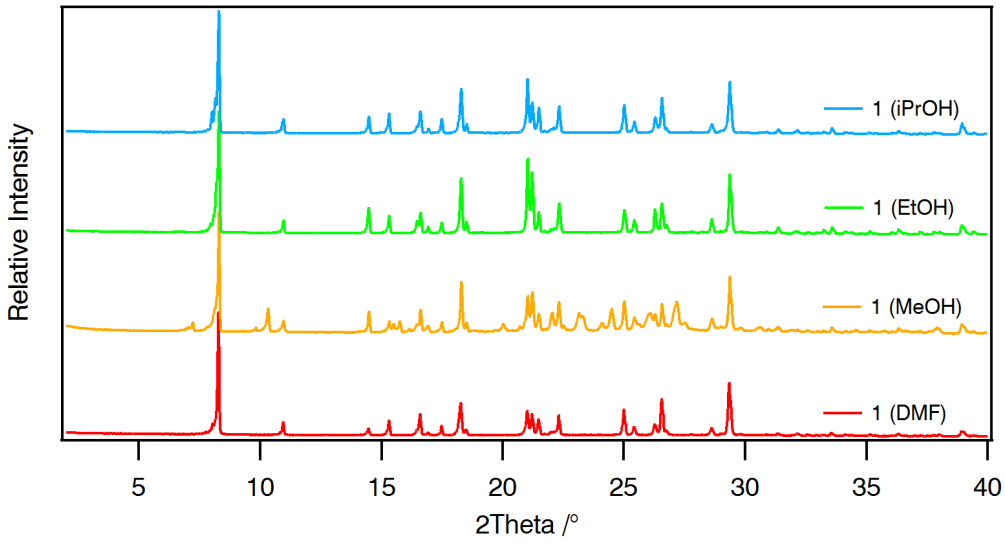

Figure SI23. PXRDs of **1** after soaking in: (*from bottom to top*) DMF, MeOH, EtOH and *i*PrOH for **1** week.

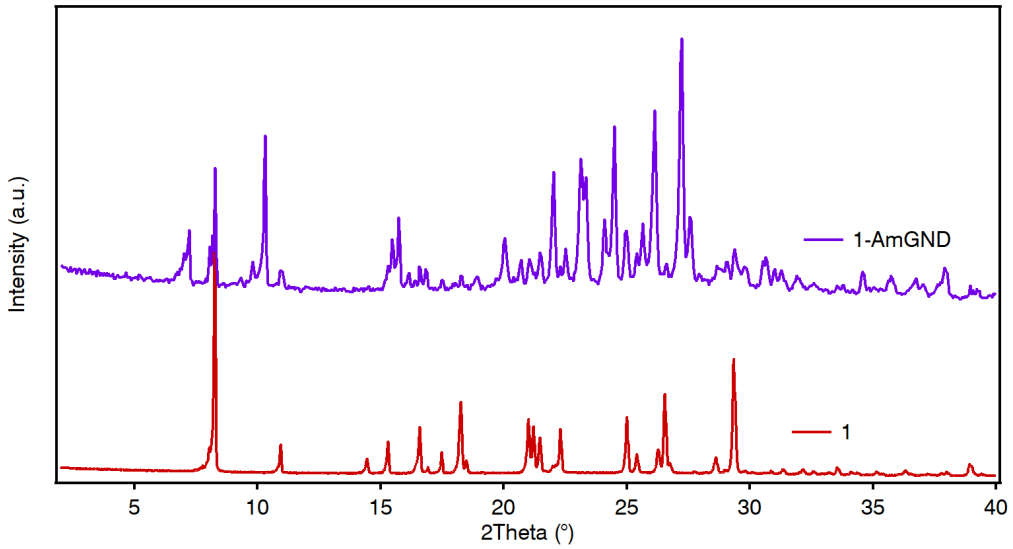

Figure SI24. PXRD of **1** before and after being immersed in an $AmGND^+$ solution for 60 days

SI4. Physical characterization of compound 2

Single-Crystal X-Ray diffraction

Table SI5. Crystal data and structure refinement for **2**

	2
Identification code	CCDC1576297
Empirical formula	$C_{18}H_{24}N_8O_{10}$
Formula weight	484.38
Temperature/K	150.00(10)
Crystal system	monoclinic
Space group	$P2_1/c$
a/Å	16.8679(6)
b/Å	18.4531(7)
c/Å	7.0790(3)
α/°	90
β/°	94.738(4)
γ/°	90
Volume/Å^3	2195.92(15)
Z	4
ρ_{calc}g/cm^3	1.465
μ/mm^{-1}	1.088
F(000)	1008.0
Crystal size/mm^3	0.136 × 0.065 × 0.043
Radiation	CuKα (λ = 1.54184)
2Θ range for data collection/°	7.114 to 117.84
Index ranges	-18 ≤ h ≤ 10, -20 ≤ k ≤ 20, -7 ≤ l ≤ 7
Reflections collected	12278
Independent reflections	3136 [R_{int} = 0.0458, R_{sigma} = 0.0346]
Data/restraints/parameters	3136/0/334
Goodness-of-fit on F^2	1.152
Final R indexes [I>=2σ (I)]	R_1 = 0.0992, wR_2 = 0.3141
Final R indexes [all data]	R_1 = 0.1028, wR_2 = 0.3166
Largest diff. peak/hole / e Å^{-3}	0.74/-0.41

Refinement model description: number of restraints – 0; number of constraints – 0.

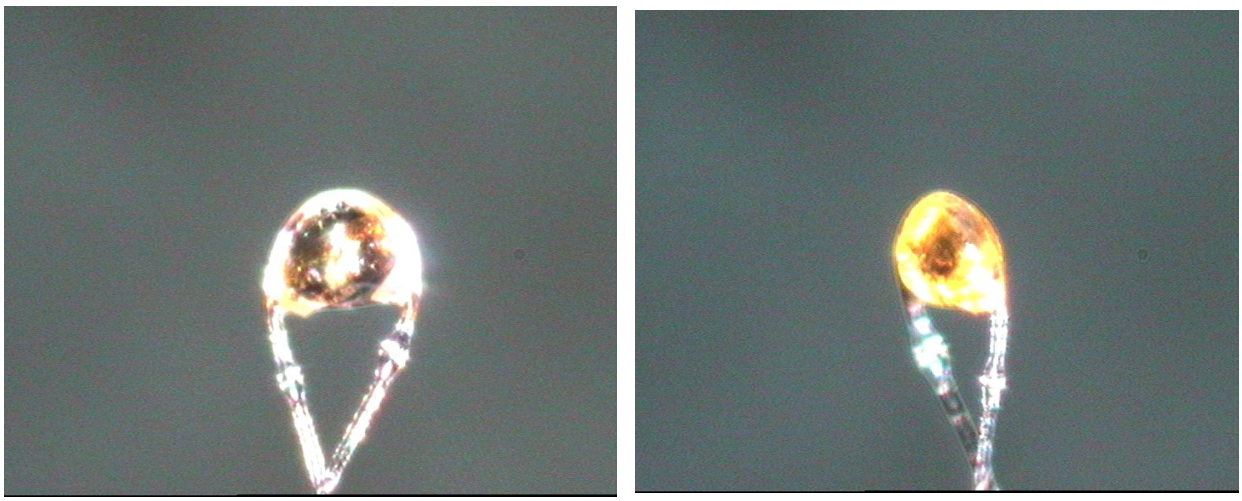

Figure SI25. Pictures for crystals of **2**

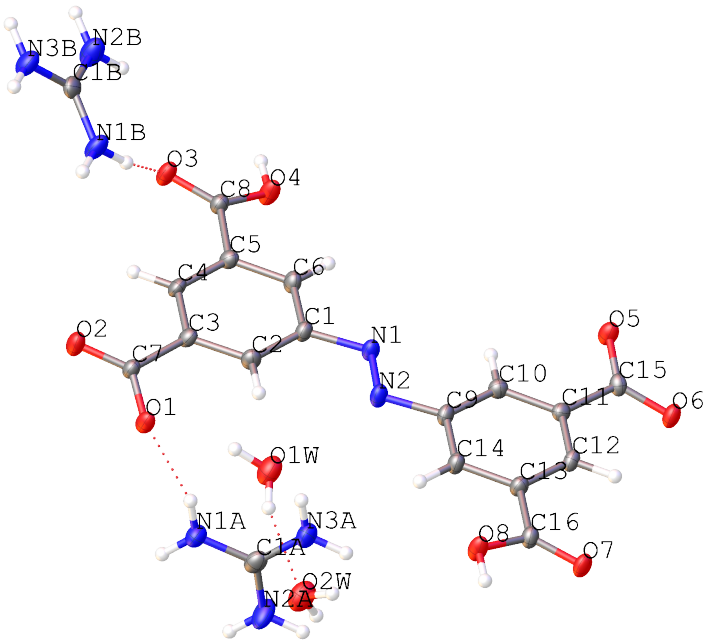

Figure SI26. Ortep representation (50% probability) of the asymmetric unit of **2**

Hydrogen bonds

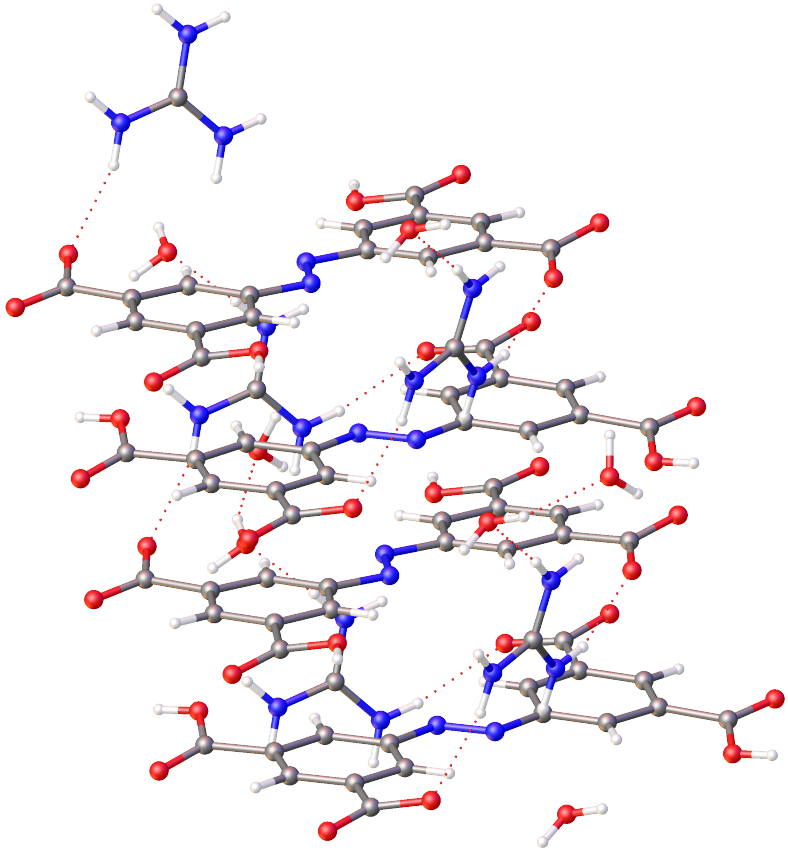

Figure SI27. Layer packing is controlled by GND^+ cations across the layers that interconnect them by acting as donor of H-bonds. See **Table SI6** for relevant H-bond distances

Table SI6. Hydrogen bonds for **2**

D	H	A	d(D-H)/Å	d(H-A)/Å	d(D-A)/Å	D-H-A/°
O4	H4	O1[1]	0.84	1.61	2.427(6)	162
O8	H8	O5[2]	0.84	1.68	2.519(6)	174
O1W	H1WA	O2W	0.85	1.96	2.749(7)	154
O2W	H2WA	O6[2]	0.85	1.93	2.720(7)	154
O1W	H1WB	O2[3]	0.85	2.23	2.938(5)	140
O2W	H2WB	O7[4]	0.85	1.97	2.803(5)	165
N15	H15A	O12	1.01(2)	1.74(2)	2.693(2)	156(2)
N15	H15B	O2[5]	0.95(2)	1.87(2)	2.738(2)	149(2)

[1]2-X,1/2+Y,3/2-Z; [2]1-X,-1/2+Y,1/2-Z; [3]2-X/-Y/1-Z; [4]1-X/-Y/1-Z; [5]X/Y/1+Z

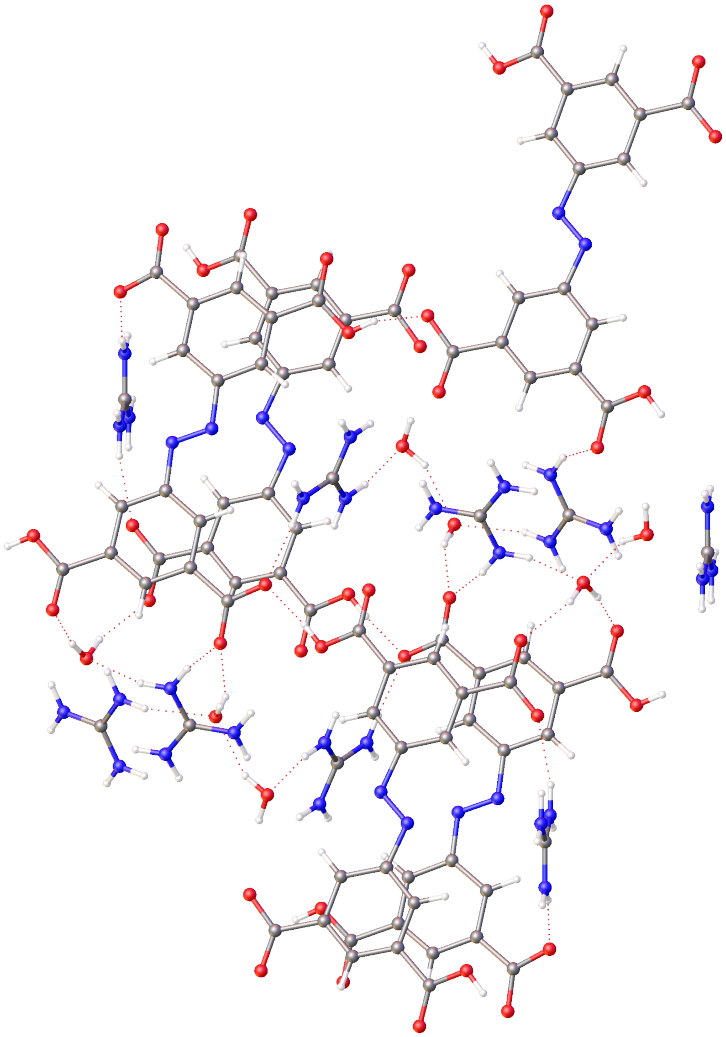

Figure SI28. Intralayer and interlayer H-bond interactions in **2**. See **Table SI6** for H-bond distances metrics

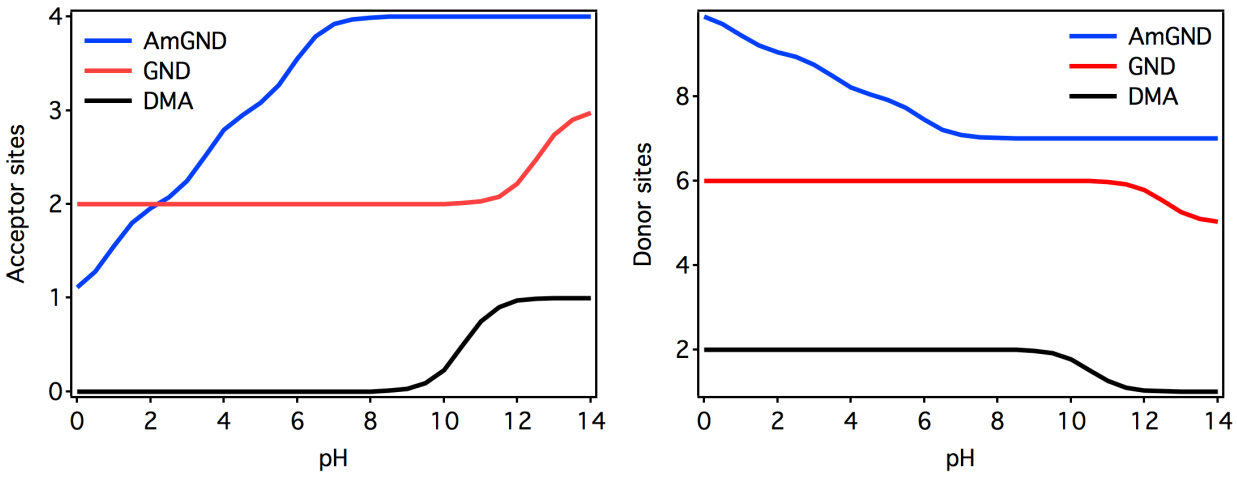

Figure SI29. Weighted average donor/acceptor multiplicities in DMA^+, GND^+ and $AmGND^+$ obtained by using H bond Donor/Acceptor Plugin, Marvin 16.8.22.0 ,ChemAxon Ltd.

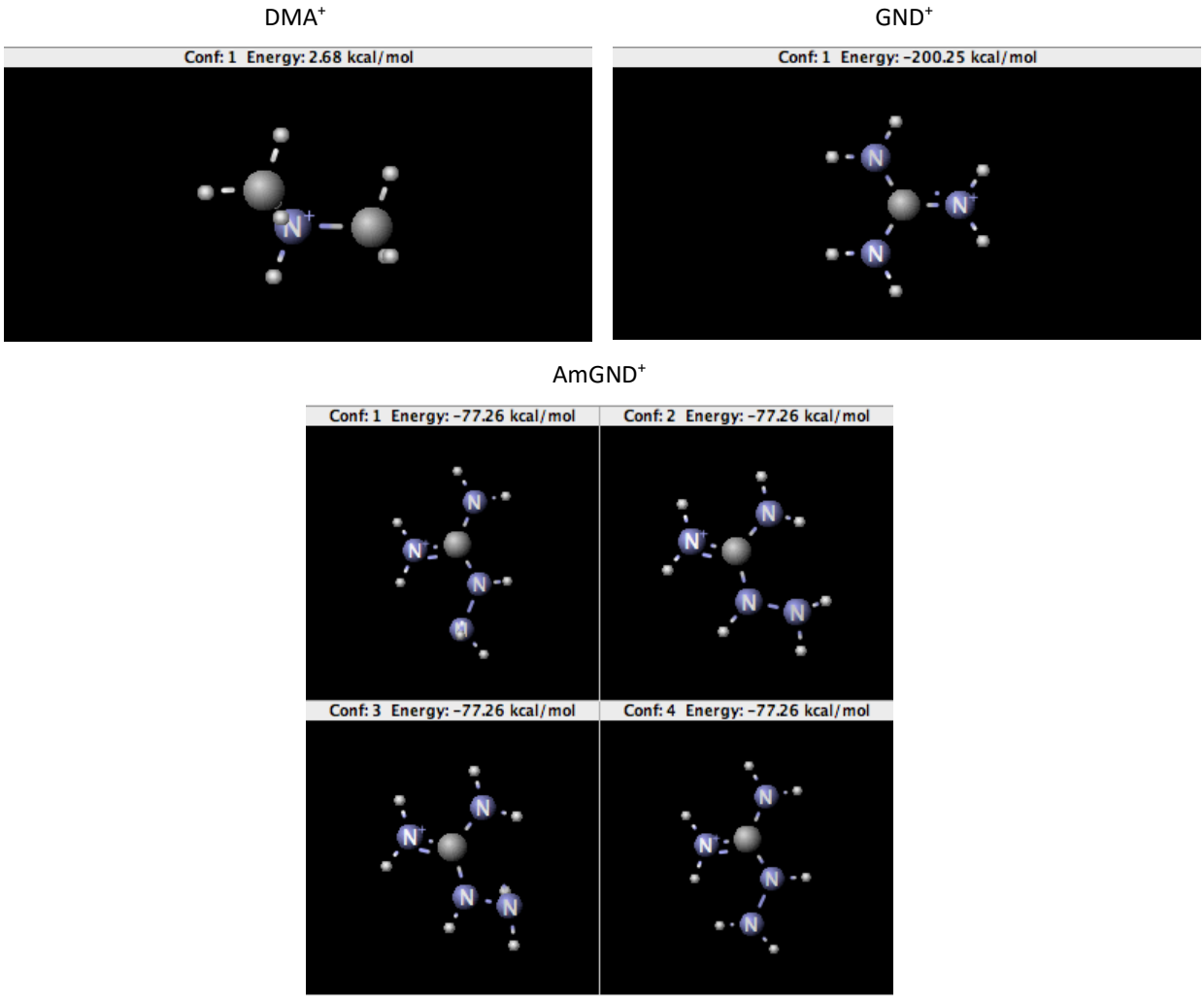

Figure SI30. Conformers of DMA^+, GND^+ and $AmGND^+$ as calculated by using the Conformer Plugin (MMFF94 force field, very strict optimization limit), Marvin 16.8.22.0 ,ChemAxon Ltd.

SI5. References.

[1]S. Ameerunisha and P. S. Zacharias, *Journal of the Chemical Society, Perkin Transactions 2*, 1995, 1679–1682.
[2]P. Dechambenoit, S. Ferlay, N. Kyritsakas and M. W. Hosseini, *J. Am. Chem. Soc.*, 2008, **130**, 17106–17113.
[3]O. V. Dolomanov, L. J. Bourhis, R. J. Gildea, J. A. K. Howard and H. Puschmann, *Journal of Applied Crystallography*, 2009, **42**, 339–341.
[4]C. Qin, Y. Feng, H. An, J. Han, C. Cao and W. Feng, *ACS Appl. Mater. Interfaces*, 2017, **9**, 4066–4073.